International Journal for Research in Engineering Application & Management (IJREAM)
ISSN : 2454-9150 Vol-05, Issue-01, April 2019

Truncation length optimization and performance evaluation of aerospike nozzle

[*]Anant Shinde, [#]Girish M Lonare, [$]Akhilesh Kumar

[*,#]Bharti Vidyapeeth College of Engineering, Navi Mumbai, India, [*]shinde.anant974@gmail.com

[$]Bhabha Atomic Research Centre, Mumbai, India, 400085, akhilesh305@gmail.com

Abstract - Aerospace industry has seen rapid growth in the last century and advances in design of exhaust nozzle have been a contributing factor. Proper design of exhaust nozzle ensures effective utilization of high energy gases coming out of the combustion chamber and improves the overall efficiency of the aircraft. There have been three major concepts in exhaust nozzle design i.e. Conical convergent divergent nozzle, Bell nozzle and Aerospike nozzle. Although Bell nozzle has been the mainstay, however, it has obvious design limitation where its efficiency reduces beyond the design pressure ratio. Aerospike design has obvious advantage of altitude compensation, but till now only a lone test flight of aerospike based aircraft has been carried out due to certain limitations and extra weight of the spike constitute a major factor. Truncation of spike length may result in loss of performance but it ensures lesser aircraft weight and it is, therefore, used for balancing among these contrasting factors. In this work, effect of spike length truncation on performance of Aerospike nozzle is studied through Computation Fluid Dynamics (CFD) based analysis which would be helpful towards further development of Aerospike nozzles for practical applications.

Keywords — Aerospike Nozzle, Computational Fluid Dynamic (CFD), Exhaust Nozzle, Aerospike Truncation, Plug nozzle, Aerospike efficiency

I. INTRODUCTION

In jet engines, expansion of combustion products and effective conversion of thermal energy into kinetic energy for propulsion is accomplished in the exhaust nozzle [1]. The exhaust nozzle, therefore, plays vital role in the overall engine performance. Variety of exhaust nozzle configurations are available today, including Conical convergent divergent, Bell-shaped, Aerospike, Truncated aerospike and Expansion-Deflection nozzles which are depicted in Fig. 1 [2].

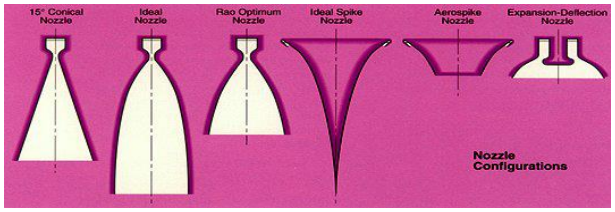


Fig. 1 Exhaust Nozzle Configurations[2]

Conical convergent divergent nozzles are rarely used due to their larger size, lower efficiency and sub-optimal performance in over and under expanded conditions [3]. Bell nozzles are most common exhaust nozzles due to their simplicity, higher thrust and lower weight due to their shorter length [4]. Bell nozzle too, however, underperforms in over and under expanded conditions. Development of exhaust nozzles with the capability of producing optimum thrust over a wide range of altitudes is highly sought after and aerospike nozzle provide this altitude compensation feature inherently. This performance improvement due to altitude compensation is curtailed, however, due to the added weight of the long spike [5]. However, by proper design the spike may be truncated which would result in slight loss in performance but significant reduction in aircraft weight.

II. AEROSPIKE CONTOUR DESIGN

The Aerospike nozzle contour in this study is designed based on method described by Youbi et.al.[6], which is an alternate method to Rao's [7] and Angelino's [8] approximation method.

The design pressure ratio was taken as 46.2 and exhaust gas temperature at inlet was taken as 500 K. The design condition is taken as 5km altitude with Ambient Pressure = 54020 Pa and Temperature as 296 K. The contour body is determined based on Prandtl-Meyer angle given by,

$$\nu = \sqrt{\frac{\gamma+1}{\gamma-1}}\tan^{-1}\sqrt{\frac{\gamma-1}{\gamma+1}(M^2-1)} - \tan^{-1}\sqrt{M^2-1}$$

 DOI : 10.18231/2454-9150.2019.0399 © 2019, IJREAM All Rights Reserved.

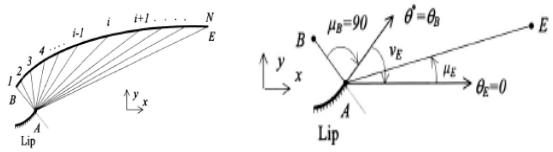


Fig.2-Aerospike contour using Youbi's method [6]

For Mach (M) = 3.0 at exit and exhaust gas with specific heat ratio (γ) = 1.21, Prandtl Meyer angle comes out to be 62.7.

For drawing the Aerospike profile, 20 ~~points~~ equi-distant Mach numbers (M_i) were taken between Mach 1.0 at throat and Mach 3.0 at exit. In Fig.2, line AB and AE, represent Mach waves at throat and exit respectively. If μ_i = Mach angle for each characteristic line, υ_i = Prandtl Meyer angle for corresponding Mach number, $\psi = (\pi/2 - \upsilon_i)$ then angle φ can be defined as $\varphi_i = [(\pi/2) - \psi - \upsilon_{i+}\mu_i]$. The angle φ_i and Expansion ratio $\varepsilon = A_{exit} / A_{throat}$ was calculated for all 20 Mach angles and rays were drawn at angle φ. On these rays, intercepts of characteristic length were taken, where characteristic length = Expansion ratio (ε_i)*Mach Number(M_i). The aerospike profile was obtained by joining tip of all the so drawn characteristic lines.

Numerical simulations

3.1 Geometry

The aerospike profile was drawn as explained in section II. The domain was selected as shown in Fig. 3, with Axial dimension more than 10D and radial extent more than 3D, where D is the nozzle inlet diameter so that results are unaffected by the exit boundary location. As the problem is axisymmetric, only the top portion of the domain was designed as a 2D axisymmetric domain. Five models were designed having full, 50%, 40%,30% and 25% aerospike length respectively.

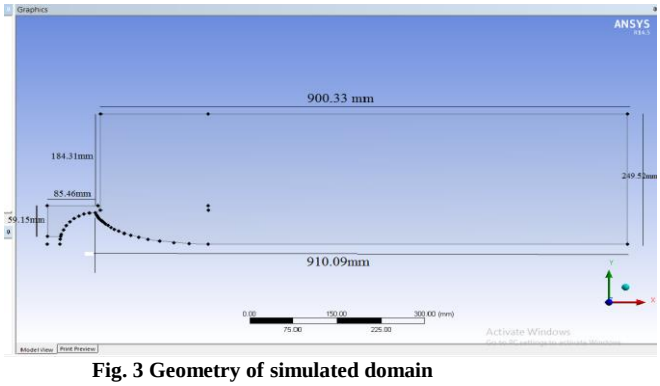


Fig. 3 Geometry of simulated domain

3.2 Meshing

Mapped face meshing was adapted and is displayed in figure 4. Mesh and domain independence studies were carried out. The generated mesh has a skewness of 0.44.

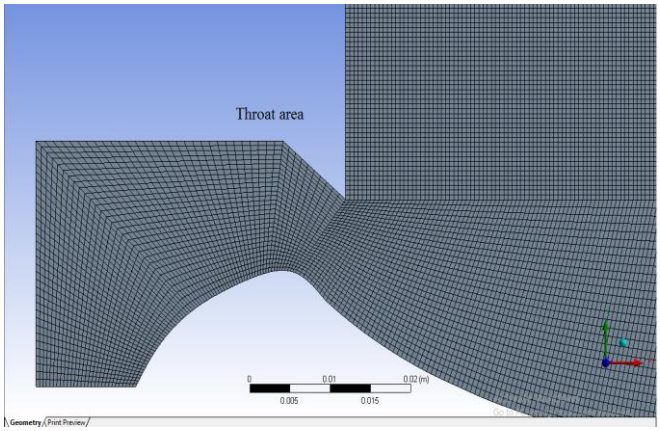


Fig. 4 Mesh around the Aerospike contour

3.3 Solver

A density-based solver with implicit formulation and k-ω SST turbulence model has been used with pressure inlet and pressure outlet boundary conditions.

III. Results and Discussions

4.1 Flow field simulation

Various phenomenon observed in flow regime of supersonic aerospike nozzle are described by Ruf and McConnaughey et al [9].

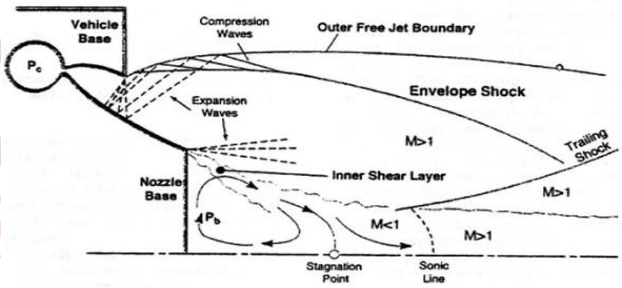


Fig. 5 Flow regime of supersonic aerospike nozzle [9]

Similar phenomenon can also be observed in the shadowgraph of actual aerospike flow obtained by Tomita et al [10] and is given in Fig. 6.

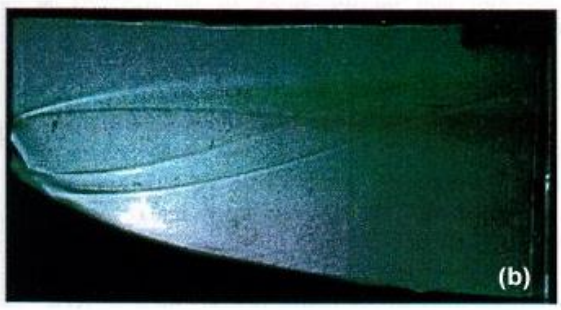


Fig. 6 shadowgraph obtained by Tomita et al [7]

Computational Fluid Dynamic (CFD) analysis was carried out for the designed geometry and all these physical phenomena of aerospike flow field like lip shock, oblique shock, Mach disc, reflected shock, recompression, recirculation, stagnation point etc. were captured in our simulation.

 DOI : 10.18231/2454-9150.2019.0399 © 2019, IJREAM All Rights Reserved.

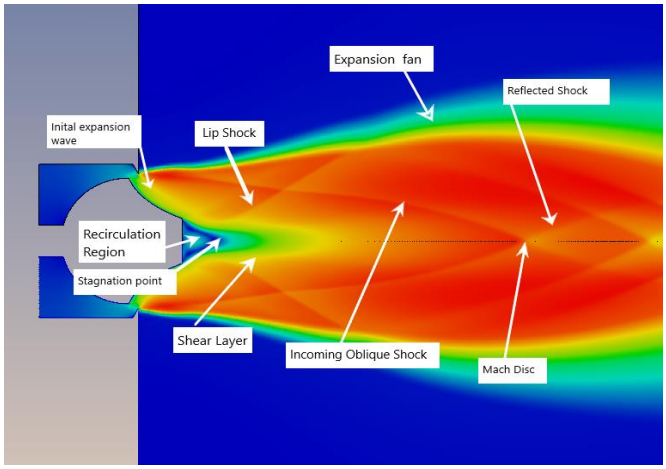


Fig. 7 flow field of the 25 % Aerospike Nozzle

4.2 Velocity contours

Velocity contours for full length aerospike, 50%, 40%, 30% and 25% aerospike nozzles were obtained and are given in Fig. 8 to Fig. 12. The comparison of axial velocity profiles and Mach profiles for these models is plotted in Fig. 13 and Fig. 14 respectively. The mass averaged surface integrals of velocity at exit are plotted in Fig. 14.

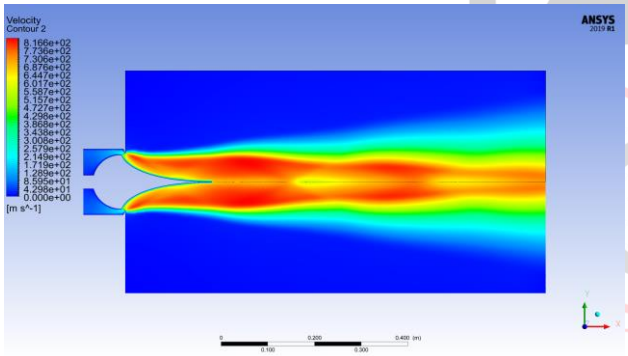


Fig. 8 Velocity contour, full Aerospike

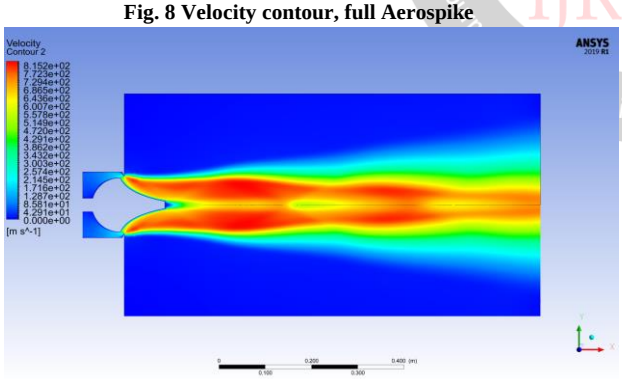


Fig. 9 Velocity contour, 50% Aerospike

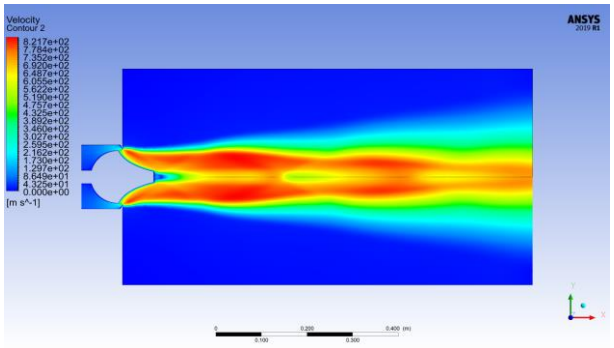


Fig. 10 Velocity contour, 40% Aerospike

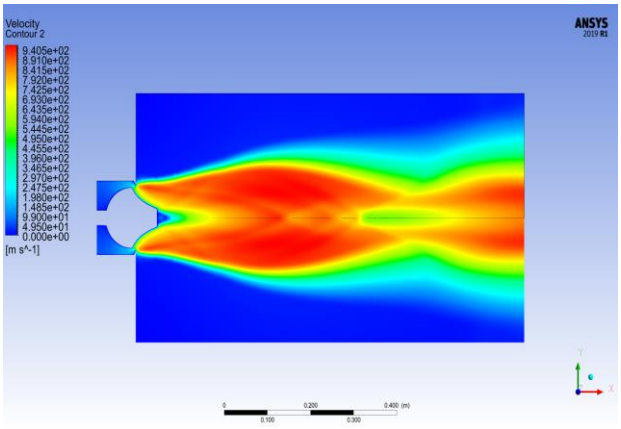


Fig. 11 Velocity contours, 30% Aerospike

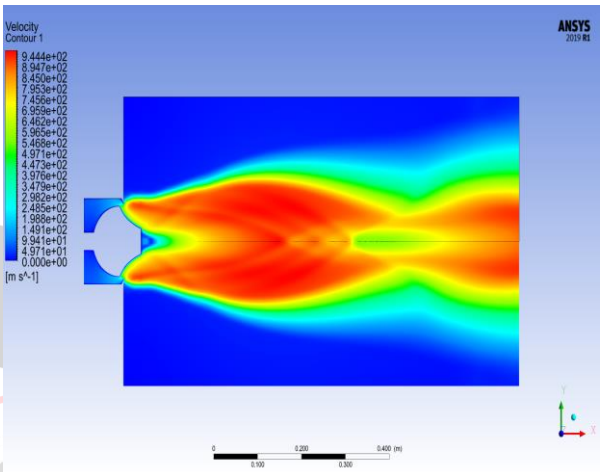


Fig. 12 Velocity contour, 25% Aerospike

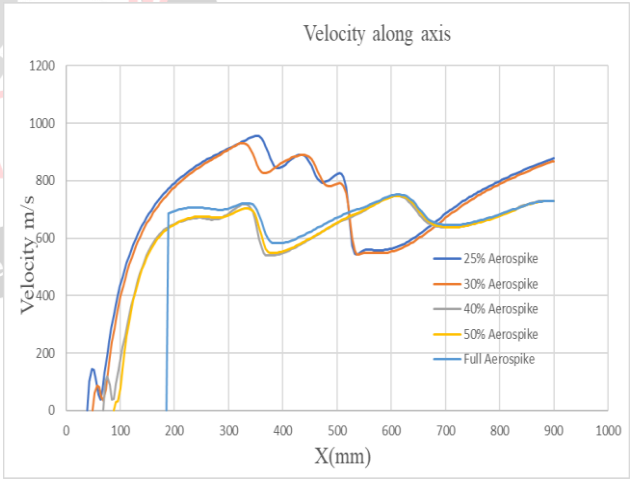


Fig. 13 Velocity along axis

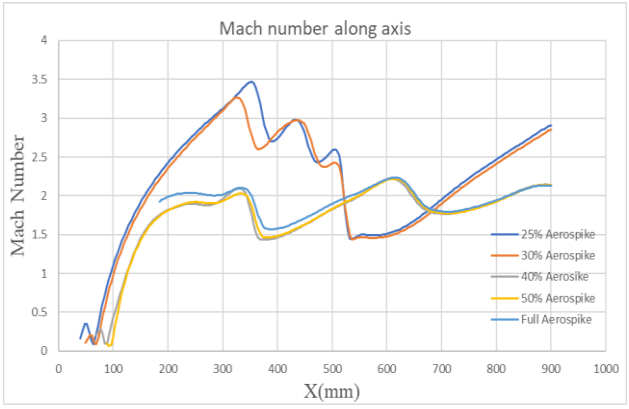


Fig. 14 Mach No. along axis

 DOI : 10.18231/2454-9150.2019.0399 © 2019, IJREAM All Rights Reserved.

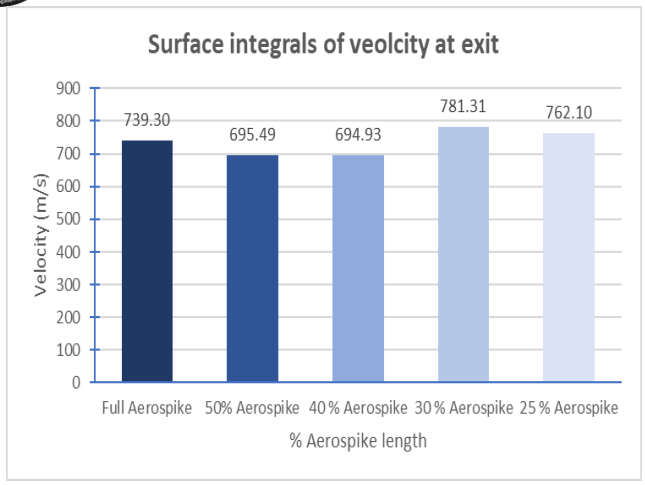


Fig. 15: Surface integral of Velocity at exit

Fig 8 to Fig 10 indicate that for full, 50% and 40 % aerospike design, only two distant shocks are present., whereas, From Fig11 and Fig. 12, it is observed that for the 30% and 25% aerospike design, two small contiguous oblique shocks take place, followed by a larger shock which bring down the velocity significantly. These shocks are clearly evident in Fig. 13 and Fig. 14 as region of sudden drop in velocity and Mach values. More number of shocks in the flow field imply more losses in kinetic energy and signify poor flow-field beyond 40% truncation. It can be observed in Fig. 15 that exit velocity of 781.3 m/s is highest for 30% aerospike nozzle whereas it is least for 40% aerospike nozzle. Velocity at exit is higher for shorter nozzles, due to the presence of Prandtl Meyer expansion fan at the edges of the truncated nozzle base, which pushes the flow away from the axes and results in wider shock diamonds.

4.3 Pressure contours

Pressure contours for full aerospike, 50%, 40%, 30% and 25% length aerospike nozzles are obtained and presented from Fig. 16 to Fig. 20. The comparison of pressure profiles along the axis for these models is plotted in Fig. 21. The mass averaged surface integral of pressure at the exit are plotted in Fig. 22.

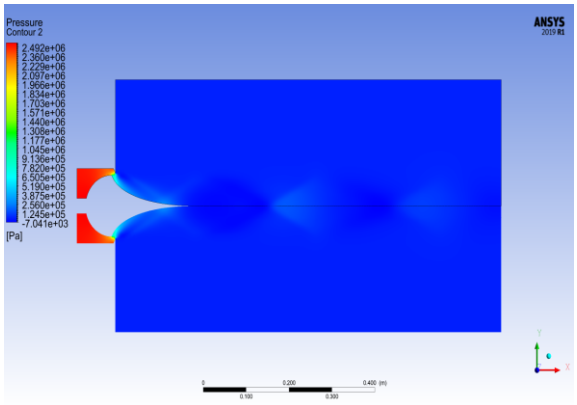


Fig. 16 Pressure contours, Full Aerospike

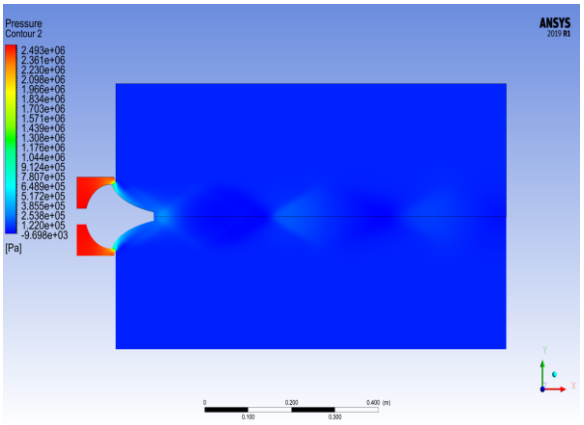


Fig. 17 Pressure contours, 50% Aerospike

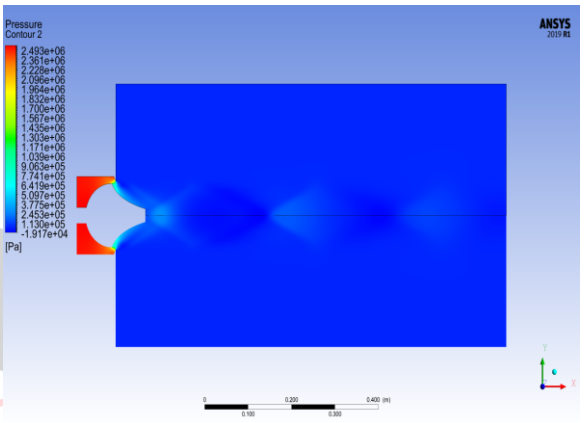


Fig. 18 Pressure contours, 40% Aerospike

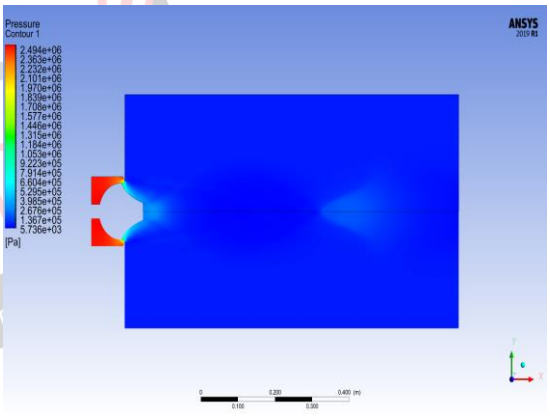


Fig. 19 Pressure contours, 30% Aerospike

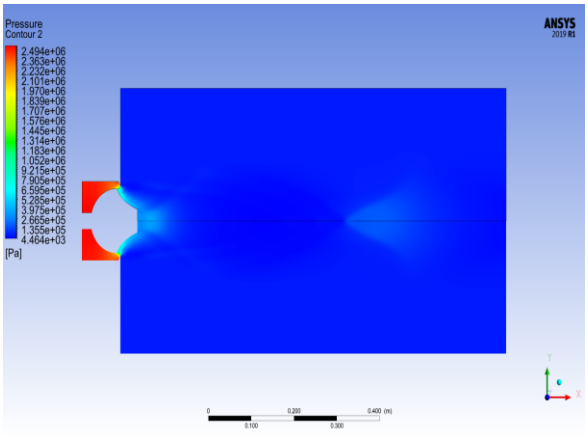


Fig. 20 Pressure contours, 25% Aerospike

 DOI : 10.18231/2454-9150.2019.0399 © 2019, IJREAM All Rights Reserved.

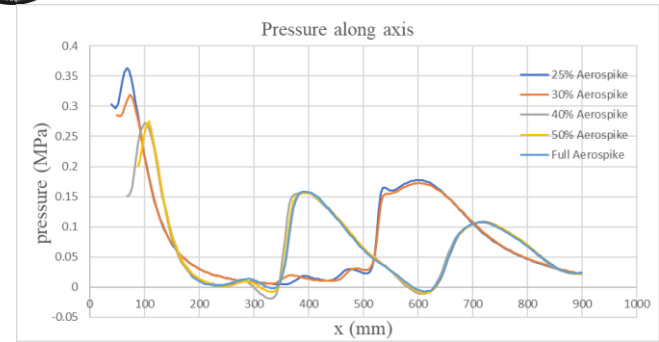


Fig. 21 Pressure along axis graph of Pressure contour

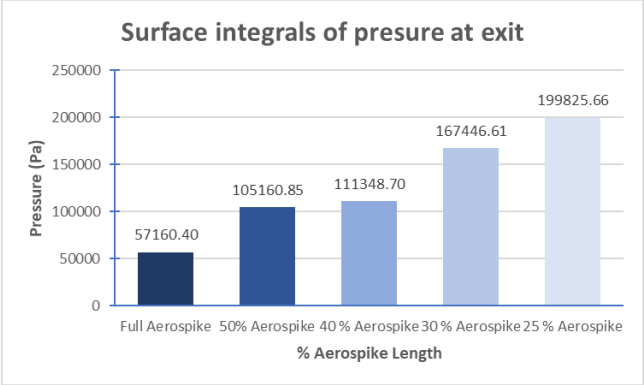


Fig. 22 Surface integral of Pressure at exit

From Fig. 16 to Fig. 20, the trailing shocks or lip shocks are visible as regions of relatively higher pressure adjacent to the aerospike profile. The oblique shocks are also visible in these figures as well as Fig. 21 as the region of steep ascending pressure values. The surface integrals of pressure at exit in Fig. 22 indicates that exit pressure is lowest for full aerospike nozzle and increase as the truncation in increased. This is due to the fact that gases are fully expanded in case of full aerospike nozzle, whereas exit pressure increases for truncated models due the presence of lip shocks and trialing shocks at nozzle base tip.

4.4 Thrust performance for truncation models

Higher thrust is desirable for any exhaust nozzle and to evaluate the performance of the models, surface integral of thrust for the truncation models are depicted in fig 23.

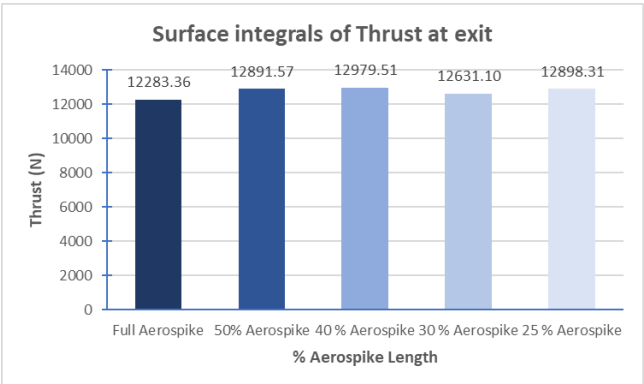


Fig. 23 Surface integral of Thrust

It can be observed that highest thrust is obtained in case of 40% aerospike nozzle. This is due to the fact that as nozzle truncation is increased, the exit pressure increases due to the presence of trailing shock at nozzle base tip, which is also elaborated in Fig 22. The increase in exit pressure is significant compared to the increase in velocity for truncated models elaborated in fig 21. This implies that as the truncation is increased, pressure component of thrust dominates the kinetic energy term of the thrust equation. 40% aerospike provides the higher thrust due to the tradeoff between these two components of thrust and therefore represents optimal design.

4.5 Performance evaluation of optimized aerospike nozzle

The nozzle was designed for 5km altitude, with ambient pressure as 54020 Pa, and ambient temperature as 296K. Performance of the optimum 40 % aerospike nozzle is compared for design condition, over expanded as well as under expanded condition. Ground level with 101325 Pa ambient pressure and 300 K ambient temperature is taken as over expanded condition whereas 10 km altitude with ambient pressure as 28095 Pa and ambient temperature as 224 K, is taken as under expanded condition. The velocity contours for design condition are already shown in Fig. 10. Velocity contours for over and under expanded condition are plotted in Fig 24 and Fig. 25 respectively.

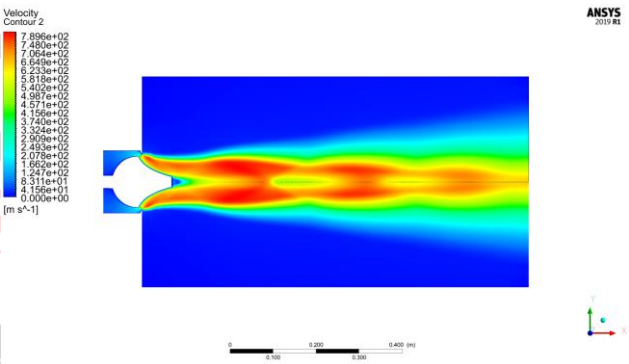


Fig. 24. Velocity contours, Over-expansion Aerospike

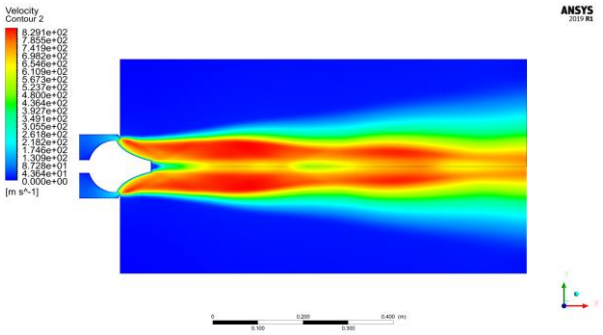


Fig. 25 Velocity contours, Under -expansion Aerospike

The comparison of mass averaged surface integrals of velocity is given in Fig 26. The velocity is highest for design condition followed by under and over expanded condition.

 DOI : 10.18231/2454-9150.2019.0399 © 2019, IJREAM All Rights Reserved.

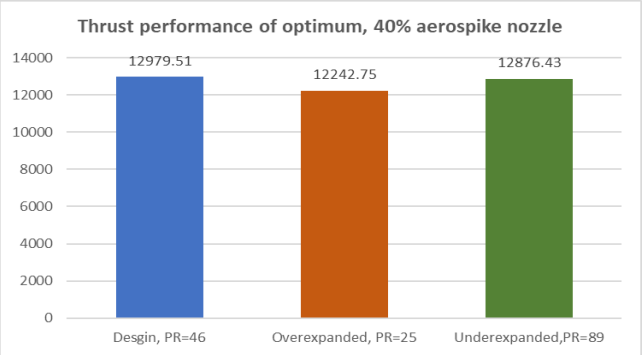


Fig. 26 Thrust performance of 40% Aerospike nozzle for design, over and under expanded condition

Efficiency of the optimized aerospike nozzle is also evaluated for design, over as well as under expanded conditions and the comparison is given in Fig. 27. It can be observed that there is only slight variation in efficiency from 34.38% to 37.76% over a wide range of operating condition i.e. from pressure ratio 15 to pressure ratio 45, which indicates superiority of aerospike design.

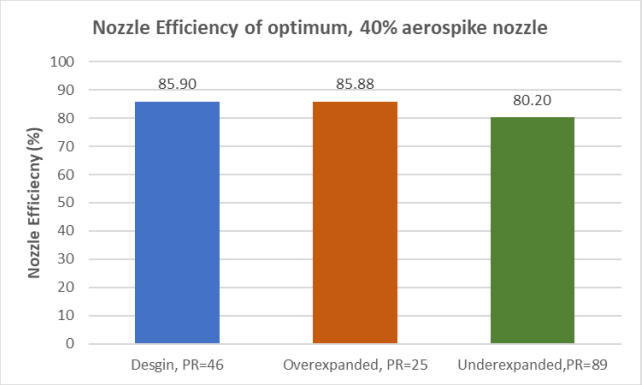


Fig. 27 Efficiency of 40% Aerospike nozzle for design, over and under expanded condition.

IV. CONCLUSION

An aerospike nozzle is designed to achieve Mach 3 at exit using Approximation method and all the physical phenomena of an aerospike flow field are captured in the simulation results. Five models are compared where the aerospike is truncated from full length to 50, 40, 30 and 25% of its original length. As the length is reduced, expansion of flow reduces accordingly, which results in lesser velocity or alternatively enhanced pressure. Nozzle performance, however, is judged based on the thrust generated by the nozzle and it is observed that thrust is highest for 40% aerospike nozzle which indicates optimum design. This happens as the base pressure thrust compensates the loss of thrust due to reduced spike length and 40% aerospike represents the trade-off condition among the two effects. Besides, more no. of shocks occurs in the flow field for truncation beyond 40% length which also contribute to poor thrust performance. The superiority of this optimized aerospike nozzle is also demonstrated over a wide range of operating conditions from ground level to 10km altitude. The aerospike nozzle gives about 5 % higher efficiency in over expanded condition compared to under expanded condition, which imply significant fuel savings at the startup phase of the aircraft.

REFERENCES

[1] Claire Sores, “Gas Turbines: A handbook of Air, Sea and Land applications”, (Second Edition), 2015, pp. 1-40

[2] R.A. O’Leary and J. E. Beck., “Nozzle Design”. Rocketdyne’s Engineering Journal of Power Technology, 1992.

[3] Chang-Hui Wang∗, Yu Liu, Li-Zi Qin, "Aerospike nozzle contour design and its performance validation", Acta Astronautica 64 (2009) pp. 1264 – 1275

[4] http://www.aerospaceweb.org/design/aerospike/shapes.shtml

[5] “Liner Aerospike Engine-Propulsion for the X-33 vehicle” , NASA Fact sheet No. FS-2000-09-174-MSFC, 08/2000

[6] Toufik Zebbiche and ZineEddine Youbi, “Supersonic Plug Nozzle, Design and Comparison to the Minimum Length Nozzle Configuration”. KSAK International journal, Vol.7, No.1, May 2006.

[7] G. V. R. Rao, “Exhaust nozzle contour for optimum thrust,” Journal of Jet Propulsion, Vol. 28, no. 6, pp. 377-382, 1968.

[8] Angelino G., “Approximation Method for Plug Nozzle Design”, AIAA Journal, Vol. 2, No. 10, Oct. 1964, pp. 1834-1835

[9] J. Ruf, P McConnaughey “The plume physics behind Aerospike nozzle altitude compensation and slipstream effect.”, 3rd Joint Propulsion Conference and Exhibit, Joint Propulsion Conference,1997

[10] Takeo Tomita, Mamoru Takashi, Takuo Onodera and Hiroshi Tamura, “Visualization of shock wave interaction on the surface of aerospike nozzles.”,34th AIAA/ASME/SAE/ASEE Joint Propulsion Conference and Exhibit, Cleveland, OH, USA, 1998

 DOI : 10.18231/2454-9150.2019.0399 © 2019, IJREAM All Rights Reserved.